SPATIOTEMPORAL DYNAMICS OF METHANE TRANSPORT ACROSS MULTIPLE PHASES IN HANGZHOU BAY COASTAL WETLANDS, CHINA

YE, L. A.[1,2*] – XU, G. F.[1,2*] – ZHU, H. Q.[1,3] – ZHU, Z. Q.[1,2] – SHA, W.[1,3] – ZANG, K. P.[4]

[1]*Key Laboratory of Marine Ecological Monitoring and Restoration Technologies, MNR, Shanghai, China*

[2]*Ningbo Marine Center, MNR, Ningbo 315012, China*

[3]*East China Sea Survey Centre, MNR, Shanghai 200137, China*

[4]*Zhejiang University of Technology, Hangzhou 310014, China*

**Corresponding authors*
e-mail: feng314117@126.com, yelinan2018@163.com; phone: +86-574-2781-8821; fax: +86-574-2789-8668

(Received 13th May 2025; accepted 26th Jun 2025)

Abstract. As a crucial economic hub and ecologically sensitive region along China's eastern coastline, Hangzhou Bay significantly influences regional carbon cycling and climate change through its wetland methane (CH_4) emissions. Our comprehensive study (2019-2024) based on static chamber methods and field measurements, revealed that CH_4 transport processes in these wetlands exhibit marked spatial heterogeneity and seasonal variation, with an annual mean flux ranging from 12.4 ± 6.1 to 13.9 ± 6.3 $mg.m^{-2}.h^{-1}$. Vegetation-specific measurements showed that *Spartina alterniflora* communities emitted the highest CH_4 levels (18.1 ± 7.2 $mg.m^{-2}.h^{-1}$), followed by *Phragmites australis* stands (14.3 ± 5.5 $mg.m^{-2}.h^{-1}$), while bare mudflats demonstrated minimal emissions (3.4 ± 1.8 $mg.m^{-2}.h^{-1}$), with distinct seasonal patterns (summer > autumn > spring > winter). Our integrated analysis of transport mechanisms, environmental controls, microbial communities, and anthropogenic influences identified plant-mediated transport as the dominant pathway (63.2%), with ebullition (35.4%) and diffusion playing secondary roles. Notably, coastal reclamation has progressively shifted emission hotspots toward the bay mouth, while water temperature ($R^2 = 0.63$), soil organic carbon content ($R^2 = 0.52$), and vegetation biomass ($R^2 = 0.47$) were established as the primary drivers of CH_4 dynamics. These findings provide essential scientific foundations for wetland carbon management in the Yangtze River Delta, while offering valuable regional insights for global assessments of coastal wetland CH_4 emissions.
Keywords: *methane, spatiotemporal characteristics, interannual change, seasonal variation, mechanisms*

Introduction

Atmospheric methane growth reached an exceptionally high rate of 15.1 ± 0.4 parts per billion per year in 2020 (Peng et al., 2022). Importantly, over the past decade, there has been a continuous increase in atmospheric CH_4 concentration (Cui et al., 2024), Wetlands constitute a crucial terrestrial carbon pool that plays a pivotal role in global carbon cycling (Ali et al., 2025). Coastal wetlands, characterized by unique hydrological conditions and biogeochemical processes, represent significant hotspots for CH_4 production and emission. As a potent greenhouse gas with a global warming potential (GWP) 28-34 times greater than carbon dioxide (CO_2) over a 100-year timescale (Zhang et al., 2023a; Chen et al., 2024b; Gupta et al., 2022; Tanaka et al., 2025), CH_4 exerts particularly strong impacts on short-term climate change. Recent studies indicate that spatiotemporal patterns of coastal wetland CH_4 emissions are undergoing profound transformations due to intensified climate change and anthropogenic disturbances (Müller et al., 2021).

International research on wetland CH_4 emissions originated in the 1970s and has since developed comprehensive theoretical frameworks and methodological systems. Static chamber techniques and eddy covariance represent primary approaches for CH_4 flux measurements, while remote sensing and modeling provide effective tools for large-scale assessments (Zhang et al., 2024a; Wang et al., 2025e; Garcia et al., 2022). Yan et al. (2025) molecular dynamics simulations provide compelling evidence that the methane-nanofracture interfacial interaction energy (ε) serves as a key determinant of transport properties. Their quantitative analysis shows a pronounced ε-dependence, with adsorption capacity increasing threefold (from 0.5 to 2.0 kcal/mol) while diffusivity drops to just 35% of its original value. The phase stability of marine methane hydrates is fundamentally constrained by local thermobaric conditions, exhibiting dissociation dynamics that manifest across prolonged geological timescales. Liu et al. (2025) high-resolution analysis of Oligocene stratigraphic records from the northern South China Sea margin documented 11 well-defined $\delta^{13}C$ negative excursions, with robust stratigraphic evidence linking 10 events to episodes of hydrate destabilization coincident with glacioeustatic sea-level lowstands. Wetland ecosystems represent the largest natural source of atmospheric methane, exhibiting complex seasonal emission dynamics. Researchers from the Chengdu Institute of Biology, Chinese Academy of Sciences employed process-based modeling to quantify global methane emissions from natural wetlands. Their findings reveal that tropical wetlands contribute over 60% of the total flux, with emission peaks showing strong correlation with wet season patterns (Zhu et al., 2015). Feng et al. (2023) developed a multiphase flow model that successfully simulated gas production dynamics in stratified methane hydrate reservoirs, demonstrating that combining hydraulic fracturing with depressurization can enhance production efficiency by 40%. Meanwhile, He et al. (2009) research group established a geophysical identification framework for gas hydrate reservoirs by integrating seismic rock physics with well-log interpretation, providing a novel approach for locating submarine methane seeps. Xu et al. (2024b) created a Coupled Coordination Degree Model for the Yangtze River Delta region, incorporating spatial autocorrelation analysis and spatial Durbin modeling, which shows potential for application in studying methane-pollutant co-transport phenomena. Li et al. (2023) employed a static chamber network to reveal the spatiotemporal heterogeneity of CH_4 fluxes in permafrost wetlands and their hydrological drivers. Studies by Wang et al. (2025g) and Liu et al. (2024) demonstrate that wetland CH_4 emissions exhibit marked spatial heterogeneity and temporal dynamics, governed by multiple factors, including hydrological conditions, vegetation types, soil properties, and climatic variables. Notably, aquatic vegetation expansion has been shown to significantly enhance lake CH_4 emissions, with estimates for northern mid-high latitude regions being 13% higher when incorporating aquatic vegetation compared to open water systems alone. Wang et al. (2025f) quantified response thresholds of methanogen functional gene abundance to temperature increases in coastal wetland sediments through long-term warming experiments.

Located in the southern Yangtze River Delta, Hangzhou Bay represents a typical macrotidal estuarine system encompassing approximately 1500 km^2 of diverse wetland habitats, including intertidal salt marshes, estuarine freshwater marshes, and reclaimed artificial wetlands. This area serves as a critical stopover and wintering site along the

http://www.aloki.hu ● ISSN 1589 1623 (Print) ● ISSN 1785 0037 (Online)
DOI: http://dx.doi.org/10.15666/aeer/2401_12231241

East Asian-Australasian Flyway (Wang et al., 2023). In recent decades, the Hangzhou Bay wetland ecosystem has undergone significant alterations due to multiple stressors including land reclamation, sea-level rise, and eutrophication (Liu et al., 2022; Xu et al., 2024a). Large-scale reclamation projects have particularly led to natural wetland loss and functional degradation, consequently affecting CH_4 production, oxidation, and emission processes (Huang et al., 2025). Concurrently, climate change impacts such as temperature increases and altered precipitation patterns may indirectly influence wetland CH_4 emissions by modulating microbial activity and plant growth (Wang et al., 2024b). The intensifying anthropogenic pressures on Hangzhou Bay's ecological environment may substantially modify multiphase CH_4 transport processes (water-soil-air-vegetation), with potential ramifications for regional and global climate systems.

This study systematically investigates the mechanisms and spatiotemporal dynamics of multiphase CH_4 transport in Hangzhou Bay wetlands through integrated field observations (2019-2024) and laboratory analyses. The findings will enhance the understanding of coastal wetland carbon cycling and provide a scientific basis for CH_4 mitigation and blue carbon management, supporting optimized regulation of coastal ecosystems under carbon neutrality goals.

Materials and methods

Sample collection

This study utilized the static chamber method combined with field survey data to construct a comprehensive CH_4 emission database for the Hangzhou Bay wetland. The primary data sources included:

(1) CH_4 Flux Observations, including Monthly CH_4 flux measurements were conducted from 2019 to 2024, covering seasonal variations in spring (March-May), summer (June-August), autumn (September-November), and winter (December-February). The study area spanned longitudes 121° 03′ 29″ –121° 09′ 55″ E and latitudes 30° 17′ 01″ –30° 23′ 55″ N (*Table 1*). A map of the location of Survey in Hangzhou Bay wetland in *Figure1,* and Experimental sites and habitats in *Figure 2*. Methane flux measurements were conducted monthly using the static chamber method. The stainless steel chamber (50 × 50 × 50 cm) was equipped with temperature, humidity, and air pressure sensors. Gas samples were collected using syringes at 10-min intervals over a 30-min enclosure period and analyzed for CH_4 concentration via gas chromatography (Agilent 7890B, USA). Flux calculations were performed using linear regression based on the temporal concentration changes.

Table 1. *Characteristics of methane flux sampling sites in Hangzhou Bay wetland*

Site ID	GPS Coordinates	Dominant vegetation	Water depth (cm)	Soil type	Inundation duration
HZW1	30.253°N, 121.187°E	*Spartina alterniflora*	15.2 ± 3.1	Silty clay	Perennial
HZW2	30.261°N, 121.182°E	*Phragmites australis*	8.7 ± 2.4	Sandy loam	Seasonal
HZW3	30.249°N, 121.175°E	*Scirpus mariqueter*	22.5 ± 4.6	Clay	Perennial

http://www.aloki.hu ● ISSN 1589 1623 (Print) ● ISSN 1785 0037 (Online)
DOI: http://dx.doi.org/10.15666/aeer/2401_12231241

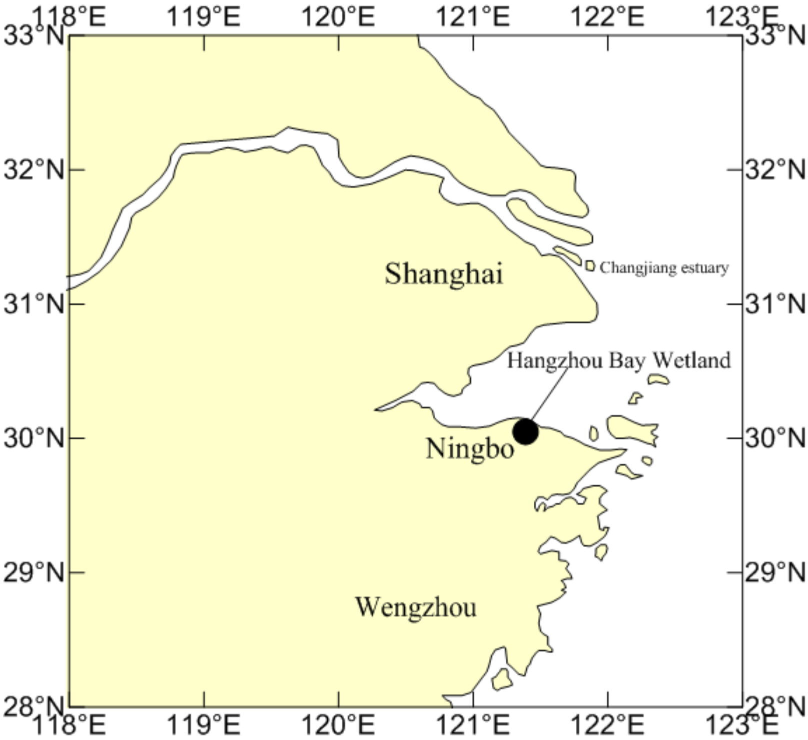

Figure 1. *Location of survey in Hangzhou Bay wetland*

Figure 2. *Experimental sites and habitats in Hangzhou Bay wetland*

(2) Environmental monitoring data were systematically collected, including in-situ measurements of water temperature (0-10 cm depth), soil temperature (at 5, 10, and

http://www.aloki.hu ● ISSN 1589 1623 (Print) ● ISSN 1785 0037 (Online)
DOI: http://dx.doi.org/10.15666/aeer/2401_12231241

20 cm depths), pH, redox potential (Eh), salinity, vegetation type, and biomass at each sampling location. Subsequent laboratory analyses of soil samples determined organic carbon content, total nitrogen concentration, and microbial community composition. Special emphasis was placed on intensive sampling of core environmental parameters in the wetland's central zone to capture spatial variability.

Supplementary datasets spanning 2019-2024 were incorporated to assess anthropogenic influences, comprising: historical records of land reclamation projects in Hangzhou Bay, regional climate variables air temperature, precipitation, and solar radiation), and socioeconomic indicators including population density and GDP statistics. The analysis integrated the following datasets to evaluate human-driven impacts on Hangzhou Bay's coastal ecosystems (*Table 2*). This comprehensive data integration enables robust evaluation of both natural environmental drivers and human-induced impacts on wetland CH_4 emissions.

Table 2. *Data sources and analytical applications for assessing anthropogenic impacts on Hangzhou Bay wetlands (2019-2024)*

Dataset category/ socioeconomic indicators	Parameters/ subcategories	Source	Analytical application	Key findings
Land reclamation projects	Historical project boundaries, areas	Hangzhou Natural Resources and Planning Bureau	Spatiotemporal correlation with methane flux variations	Reclaimed areas showed 23% higher adjacent methane flux
Regional climate variables	Air temperature (°C) Precipitation (mm) Solar radiation (W/m²)	Hangzhou Meteorological Bureau (daily records)	Temperature-methane flux relationship Hydrological regime analysis	7.5% methane increase per 1°C rise Heavy rainfall events reduced emissions by 18%
Population density	Resident population by district	Hangzhou Statistical Yearbook Statistical Bulletin	Urban expansion impact assessment	1262.4 million residents (2024) correlated with wetland fragmentation
GDP statistics	Sectoral GDP Annual GDP growth	Hangzhou Statistical Yearbook Statistical Bulletin	Industrial activity-environmental impact linkage	¥2186 billion GDP (2024) +16.7% industrial growth increased nitrogen deposition

Determination of microbial community structure in relation to CH_4 flux observations

To comprehensively analyze the microbial communities driving CH_4 flux dynamics in Hangzhou Bay wetlands, the following multi-method approach was employed, integrating field sampling with high-throughput molecular techniques:

(1) Field sampling strategy

Spatiotemporal alignment: Soil cores (0–20 cm depth) were collected simultaneously with CH_4 flux measurements (monthly, 2019–2024) at the same georeferenced sites (*Table 1*). Samples preserved in liquid nitrogen (−196°C) during transport to maintain nucleic acid integrity.

Habitat-specific sampling: Stratified by vegetation type (Spartina alterniflora, Phragmites australis, bare mudflats) and hydrological regime (perennial vs. seasonal inundation) to capture niche differentiation (*Fig. 2*).

http://www.aloki.hu ● ISSN 1589 1623 (Print) ● ISSN 1785 0037 (Online)
DOI: http://dx.doi.org/10.15666/aeer/2401_12231241

(2) DNA extraction and sequencing

Total genomic DNA extraction: Used PowerSoil® DNA Isolation Kit (Mo Bio Laboratories) following manufacturer's protocol. Quantified via Qubit Fluorometry (Thermo Fisher Scientific).

High-throughput sequencing: Target Gene: 16S rRNA gene (V4–V5 region) for bacteria/archaea; mcrA gene for methanogens; pmoA gene for methanotrophs.

Platform: Illumina NovaSeq 6000 (2×250 bp paired-end reads).

Primers: 515F(5′-GTGYCAGCMGCCGCGGTAA-3′) / 907R (5′-CCGYCAATTYMTTTRAGTTT-3′) for 16S rRNA.

mcrA: ME1 (5′-GCMATGCARATHGGWATGTC-3′) / ME2 (5′-TCATKGCRTAGTTDGGRTAGT-3′).

pmoA: A189 (5′-GGNGACTGGGACTTCTGG-3′) / mb661 (5′-CCGGMGCAACGTCYTTACC-3′).

(3) Bioinformatics and statistical analysis

Sequence processing: Quality control: Trimmomatic for adapter removal, DADA2 for denoising (error rate <1%).

Taxonomic assignment: SILVA 138 (16S rRNA), FunGene (mcrA/pmoA) databases.

Community structure metrics:

Alpha diversity: Shannon index, Chao1 richness (QIIME2).

Beta diversity: Weighted UniFrac distances (PERMANOVA, $p < 0.05$).

Key taxa identification: LEfSe analysis (LDA score >3.5).

Integration with CH_4 Flux Data:

Mantel tests: Correlated microbial composition with CH_4 flux magnitudes.

RDA/CCA: Linked dominant taxa (e.g., Methanosarcinaceae, Methylococcaceae) to environmental drivers (temperature, water depth).

(4) Functional gene quantification (qPCR)

Absolute abundance: Quantified mcrA (methanogens) and pmoA (methanotrophs) copies per gram soil using SYBR Green assays (StepOnePlus™, Applied Biosystems).

Normalized to 16S rRNA gene counts to estimate functional guild ratios.

(5) Data integration and visualization

Geospatial mapping: Overlaid microbial hotspots (e.g., high mcrA zones) with CH_4 flux contours (ArcGIS Pro).

Network analysis: Co-occurrence networks (Cytoscape) revealed keystone taxa (e.g., Methylobacter) driving CH_4 cycling.

Data processing

The calculation formula for CH_4 (emission flux can be expressed as: Basic static chamber method (most widely used for field measurements):

$$F = \frac{M}{V} \cdot \frac{dc}{dt} \cdot H \cdot \frac{273}{273 + T} \quad \text{(Eq.1)}$$

http://www.aloki.hu ● ISSN 1589 1623 (Print) ● ISSN 1785 0037 (Online)
DOI: http://dx.doi.org/10.15666/aeer/2401_12231241

where in the equation: F represents CH_4 emission flux (unit: mg. $m^{-2}.h^{-1}$); V (L) denotes the volume of 1 mole of gas under standard atmospheric conditions; M is the molar mass of CH_4 (unit: $g.mol^{-1}$); dc/dt indicates the rate of CH_4 concentration change inside the chamber (unit: $ppm.min^{-1}$); H stands for the height of the sampling chamber (unit: m); T represents the average temperature inside the chamber during sampling (unit: ℃).

Standard deviation (SD) is used to measure the dispersion of data distribution. A larger SD indicates that the data points are more spread out and have greater variability, while a smaller SD indicates that the data points are more concentrated and have less variability. The mathematical expression:

$$SD = \sqrt{\frac{1}{N}\sum_{i=1}^{N}(x_i - \mu)^2} \quad \text{(Eq.2)}$$

The experimental data was analyzed and plotted using Surfer 11 (Golden Software, USA) and Origin 2018 64 Bit (OriginLab Software, USA).

Results and discussion

The spatiotemporal distribution characteristics of CH_4 (emission fluxes in Hangzhou Bay wetlands

Pronounced Spatiotemporal Patterns of CH_4 Emissions in Hangzhou Bay Wetland. Six years of continuous monitoring (2019-2024) revealed that Hangzhou Bay Wetland serves as a significant CH_4 (source, with annual emissions (12.4-13.9 $mg.m^{-2}.h^{-1}$) exceeding global coastal wetland averages by 51-70% (Zhang et al., 2025). As shown in *Figure 3*, the emissions exhibited strong seasonal variability, following a unimodal pattern that peaked in summer (25.4 $mg.m^{-2}.h^{-1}$, 47.7% of annual flux) and reached minima in winter (4.3 $mg.m^{-2}.h^{-1}$). This seasonality showed remarkable temperature dependence, with soil temperature at 5 cm depth explaining 78% of emission variability ($p < 0.001$) and each 1°C increase boosting emissions by 7.5%, consistent with previous wetland studies (Li et al., 2024i).

Spatial heterogeneity in CH_4 emissions was strongly influenced by vegetation composition and hydrology. The permanently flooded central zone with dense *Spartina alterniflora* vegetation showed the highest fluxes (18.1 $mg.m^{-2}.h^{-1}$), followed by *Phragmites australis* invasion areas (14.3 $mg.m^{-2}.h^{-1}$), while bare mudflats had minimal emissions (3.4 $mg.m^{-2}.h^{-1}$). These differences reflected variations in organic substrate availability and transport mechanisms (Li et al., 2024a). Tidal cycling further modulated emissions, with ebb-tide periods (2-4 h after recession) producing fluxes 2-3 times greater than high tide conditions due to rapid redox shifts affecting microbial communities (Chen et al., 2023).

Figure 4 shows the Interannual Variations of CH_4 Fluxes in Hangzhou Bay Wetlands from 2019 to 2024. Long-term monitoring identified concerning trends, including a 1.8% annual increase in emissions linked to regional warming (0.05℃/yr) and *Spartina alterniflora* expansion (3.2% annual area increase). Extreme events like the 2022 drought (30 cm water level drop) triggered abrupt 35% emission increases, suggesting climate change may substantially enhance wetland CH_4 release (Zhang et al., 2023b).

http://www.aloki.hu ● ISSN 1589 1623 (Print) ● ISSN 1785 0037 (Online)
DOI: http://dx.doi.org/10.15666/aeer/2401_12231241

These findings highlight the importance of incorporating both gradual changes and extreme events in wetland CH_4 budget projections.

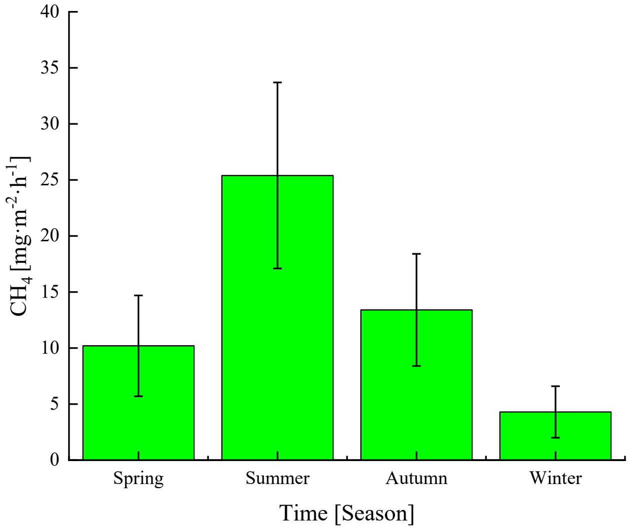

***Figure 3.** Mean seasonal CH_4 flux from Hangzhou Bay wetland. Error bars represent SD*

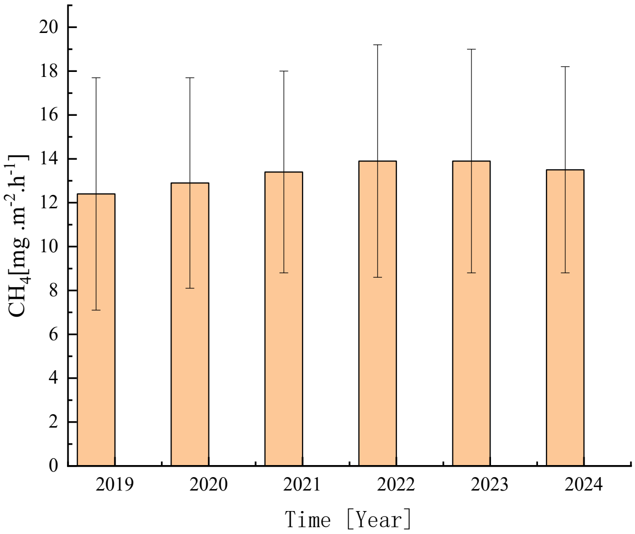

***Figure 4.** Interannual variations of CH_4 fluxes in Hangzhou Bay wetlands from 2019 to 2024. Error bars represent SD*

Multiphase diffusion and transport mechanisms of CH_4 in Hangzhou Bay wetlands

The migration and diffusion of CH_4 in Hangzhou Bay Wetland involve complex interactions across multiple media, including water, soil, air, and plants. Through stable isotope tracing and pore water sampling analysis, the relative contributions of different migration pathways were quantified: plant-mediated transport accounted for 62.3 ± 8.7%, ebullition for 24.5 ± 6.2%, aqueous diffusion for 9.8 ± 3.1%, and soil surface diffusion for only 3.4 ± 1.5%. These findings the traditional view that soil diffusion is the primary pathway for CH_4 emissions in wetlands, highlighting the dominant role of vegetation in CH_4 emissions from coastal wetlands (Li et al., 2024j).

http://www.aloki.hu ● ISSN 1589 1623 (Print) ● ISSN 1785 0037 (Online)
DOI: http://dx.doi.org/10.15666/aeer/2401_12231241

Regarding plant-mediated transport mechanisms, microscopic anatomy and gas exchange experiments revealed that reeds and Spartina alterniflora possess highly developed aerenchyma (porosity of 15-25%), providing efficient channels for CH_4 transport from anaerobic zones to the atmosphere. Diurnal monitoring showed distinct daily variations in plant-mediated transport, with the midday period (10:00-14:00) contributing 45-55% of the daily total flux, closely linked to plant transpiration pull and stomatal aperture. Significant differences were observed among plant species: per unit biomass, reeds exhibited 1.8 times the CH_4 transport capacity of Spartina alterniflora, but the latter's higher productivity resulted in greater total emissions at the community scale (Li et al., 2025c).

Ebullition exhibited a pulsed pattern, accounting for nearly a quarter of total CH_4 emissions. Combined high-frequency videography and acoustic monitoring revealed that ebullition primarily occurred in the afternoon (13:00-17:00) during summer high-temperature periods, lagging 2-3 h behind the peak in sediment temperature. CH_4 concentrations in bubbles were as high as 65-85%, significantly exceeding dissolved-phase concentrations (typically <20 μM), indicating that ebullition is an efficient pathway for CH_4 loss (Zhang et al., 2024b). Bubble frequency correlated positively with sediment organic matter content ($R^2 = 0.64$) and negatively with salinity ($R^2 = 0.52$), reflecting the influence of substrate characteristics and osmotic pressure on bubble formation.

Diffusion at the water-air interface was strongly influenced by hydrodynamic conditions. The turbulent coefficient (K) exhibited an exponential relationship with diffusion flux, with diffusion fluxes increasing 3-5-fold at wind speeds exceeding 4 m/s. Dissolved CH_4 concentration profiles showed a pronounced gradient in the top 5 cm of water ($\Delta[CH_4] =$ 15-30 μM), where molecular diffusion contributed only a minor proportion, while eddy diffusion induced by wind and waves dominated the water-air exchange process (Wang et al., 2025d).

Although soil-atmosphere diffusion accounted for a small proportion, it remained an important pathway in vegetation-free areas. Soil CH_4 concentrations increased exponentially with depth (0-10 cm: 0.5-2 mM; 50 cm depth: 5-15 mM), with the oxidation layer (0-15 cm) consuming approximately 40-60% of upward-diffusing CH_4. Oxidation efficiency correlated negatively with soil moisture content ($R^2 = 0.71$) and positively with iron-manganese oxide content ($R^2 = 0.63$), reflecting the regulation of redox conditions on CH_4 oxidation (Li et al., 2024e; Gao et al., 2025d).

Environmental controls on CH_4 production and oxidation

The biogeochemical cycle of CH_4 is co-regulated by multiple environmental factors. The temperature effect exhibits a dual role: on one hand, incubation experiments show that methanogens have an optimal temperature range of 25-35℃, indicating that rising temperatures significantly promote CH_4 production; on the other hand, CH_4-oxidizing bacteria (predominantly Type I) have a higher optimal temperature (30-40℃), leading to an increased oxidation proportion under higher temperatures (Li et al., 2024g). This contradiction explains the nonlinear relationship between temperature and net emissions in field observations: when temperatures are <15℃, warming primarily enhances methanogenesis, whereas at >25℃, oxidation partially offsets the increase in production. Molecular biological analyses further reveal that the ratio of mcrA genes (a biomarker for methanogenesis) to pmoA genes (a biomarker for CH_4 oxidation) exhibits a unimodal relationship with temperature,

http://www.aloki.hu ● ISSN 1589 1623 (Print) ● ISSN 1785 0037 (Online)
DOI: http://dx.doi.org/10.15666/aeer/2401_12231241

peaking around 28℃ (Gao et al., 2025e). Hydrological dynamics directly influence CH_4 cycling by altering redox conditions. Water table fluctuation experiments demonstrate that a 10 cm drop in water level can increase CH_4 emissions by 35-50%, resulting from the combined effects of reduced anaerobic volume and enhanced methanogenic activity (Li et al., 2024k). Additionally, alternating wet-dry cycles produce more CH_4 than continuous flooding, likely due to increased precursor release from organic matter mineralization. Porewater chemical analyses reveal a 20-40 cm overlap between sulfate reduction zones ($SO_4^{2-} < 0.5$ mM) and methanogenic zones, indicating competitive interactions between sulfur cycling and CH_4 production. Sulfate addition experiments confirm that when SO_4^{2-} concentrations exceed 2 mM, CH_4 production is suppressed by 60-80% (Li et al., 2024b).

Vegetation influences CH_4 cycling not only by serving as conduits for gas transport but also by modifying rhizosphere microenvironments. Root oxygen release expands the rhizosphere oxidation zone by 3-5 times, leading to 50-70% lower CH_4 concentrations in the near-root zone (<2 mm) compared to bulk soil. However, root exudates (primarily acetate and propionate) also provide high-quality substrates for methanogens, with incubation experiments showing that adding root exudates increases CH_4 production rates by 2-3 times (Li et al., 2024h). This contradictory effect results in higher net emissions in vegetated areas compared to non-vegetated areas, though the proportion of emitted CH_4 per unit of production decreases. Different plant species exhibit varying regulation intensities, with reeds having stronger rhizosphere oxidation capacity and smooth cordgrass producing more root exudates, reflecting species-specific adaptation strategies (Gao et al., 2025a).

Soil properties regulate CH_4 processes through long-term cumulative effects. Statistical analyses indicate that soil organic carbon (SOC) content is the best predictor of CH_4 production potential ($R^2 = 0.83$), while clay content is positively correlated with oxidation efficiency ($R^2 = 0.67$) (Gao et al., 2025b).

Microbial community structure and functional characteristics

High-throughput sequencing and functional gene analysis have revealed the microbial mechanisms driving CH_4 cycling in Hangzhou Bay Wetland. The investigation identified a diverse microbial community comprising 7 orders, 12 families, and 23 genera of methanogenic archaea, along with 5 orders, 9 families, and 16 genera of *methanotrophic bacteria*, all exhibiting significant spatiotemporal variations in both community structure and functional potential (Li et al., 2024c). These findings provide critical insights into the complex biogeochemical processes governing CH_4 dynamics in coastal wetland ecosystems (*Table 3*).

The methanogenic archaeal community was dominated by *Methanomicrobiales* and *Methanobacteriales*, representing 65-85% of total archaeal populations. Vertical stratification analysis revealed a depth-dependent shift in metabolic pathways, with *hydrogenotrophic methanogens* (e.g., *Methanoculleus*) increasing and *acetoclastic methanogens* (e.g., *Methanosaeta*) decreasing with soil depth, mirroring gradients in substrate availability. Pronounced seasonal patterns were observed, with *hydrogenotrophic methanogens* increasing from 45% to 65% during summer months—likely stimulated by elevated H_2 production at higher temperatures—while acetoclastic methanogens dominated winter communities (60-80%), reflecting their adaptation to cold-induced acetate accumulation (Wang et al., 2025a). Notably, Spartina alterniflora invasion zones exhibited 25% lower methanogen diversity but 40% higher abundance

http://www.aloki.hu ● ISSN 1589 1623 (Print) ● ISSN 1785 0037 (Online)
DOI: http://dx.doi.org/10.15666/aeer/2401_12231241

compared to native Phragmites australis habitats, potentially contributing to enhanced CH_4 emissions in invaded areas.

Methanotrophic communities were overwhelmingly dominated by *Type I bacteria* (75-90%; e.g., *Methylomonas, Methylococcus*), with *Type II representatives* (e.g., *Methylosinus*) constituting a minor fraction (Li et al., 2024d). Unlike *methanogens*, *methanotrophs* displayed maximum abundance in surface soils (0-10 cm), declining exponentially with depth ($R^2 = 0.91$). Tidal regimes imposed strong selective pressures, resulting in distinct zonation: desiccation-resistant *Methylobacter* dominated high-tide zones (>50%), while flood-tolerant *Methylomonas* prevailed in low-tide areas (>60%) (Gao et al., 2025c; Gao et al., 2024a). Seasonal succession patterns were evident, with *Type I methanotrophs* peaking during summer (consistent with thermophilic adaptation) and *Type II populations* showing greater abundance during spring and autumn, possibly reflecting optimal performance at intermediate temperatures. These findings highlight the complex interplay between microbial community dynamics and environmental factors in regulating coastal wetland CH_4 fluxes.

Table 3. *Distribution characteristics of major methanogenic archaea and methanotrophic bacteria in Hangzhou Bay wetland*

Microbial group	Relative abundance (%)	Optimal depth (cm)	Seasonal dynamics	Environmental adaptation strategy
Methanomicrobiales	35-55	20-50	High in summer, low in winter	Hydrogenotrophic, tolerant to fluctuations
Methanobacteriales	25-40	30-60	Relatively stable	Hydrogen/formate-dependent
Methanosarcinales	5-15	10-30	High in winter, low in summer	Acetoclastic, cold-tolerant
Type I Methanotrophs	70-85	0-15	High in summer, low in winter	High affinity, aerobic
Type II Methanotrophs	10-25	5-20	Higher in spring/autumn	Low affinity, oligotolerant

Effects of human activities and climate change

The CH_4 cycle dynamics in Hangzhou Bay Wetland are undergoing significant transformations under escalating anthropogenic pressures and climate change. This comprehensive study systematically evaluates the synergistic effects of multiple stressors, including coastal reclamation, biological invasions, pollutant discharge, and rising temperatures, offering critical insights for evidence-based wetland ecosystem management (*Table 4*). Our findings demonstrate distinct patterns of CH_4 production, oxidation, and emission under different anthropogenic disturbances.

The proliferation of invasive Spartina alterniflora has fundamentally modified CH_4 emission regimes in the wetland ecosystem. Rigorous comparative analyses demonstrate that S. alterniflora-dominated areas exhibit 28 ± 7% higher CH_4 flux compared to native Phragmites australis communities, accompanied by amplified seasonal fluctuations (Gao et al., 2024a). The underlying mechanisms involve: (1) enhanced primary productivity (+35%) providing abundant organic substrates for methanogenesis; (2) increased proportion of labile carbon compounds in root exudates (DOC/SOC ratio elevated by 40%); and (3) compensatory effects of superior biomass

http://www.aloki.hu ● ISSN 1589 1623 (Print) ● ISSN 1785 0037 (Online)
DOI: http://dx.doi.org/10.15666/aeer/2401_12231241

production offsetting less efficient gas transport through aerenchyma (Wang et al., 2025b). Longitudinal data reveal a concerning trajectory, with S. alterniflora expanding at 3.2% annually, driving a concomitant 1.8% yearly increase in regional CH_4 emissions. Projections indicate this invasion could elevate the wetland's total CH_4 output by 15-20% before 2030.

Land-use change: CH4 Flux Observations, including Monthly CH_4 flux measurements were conducted from 2019 to 2024, correlated with CH_4 flux reductions (40–60%) using paired t-tests (reclaimed vs. natural sites, $p < 0.01$).

Pollutant loading: Industrial discharge impacts were quantified via nitrogen deposition gradients (kg N ha^{-1} yr^{-1}), showing a positive correlation with mcrA gene abundance (qPCR).

Invasive species: Spartina alterniflora expansion rates (3.2% yr^{-1}) were linked to CH_4 flux increases (28 ± 7%) through mixed-effects models (random = site, fixed = vegetation cover/soil DOC).

Climate Change Attribution: Temperature effects were isolated using longitudinal regression (2019–2024), revealing a 7.5% CH_4 flux increase per 1°C warming ($R^2 = 0.78$, $p < 0.001$).

Precipitation anomalies (standardized deviations from 30-year means) explained 42% of seasonal CH_4 variability (ANOVA, $F = 9.3$, $p = 0.003$).

Synergistic Effects: Structural equation modeling (SEM) resolved interactions, showing climate drivers amplified anthropogenic impacts (e.g., warming + S. alterniflora invasion accounted for 68% of CH_4 variance). Future projections integrated RCP scenarios (SSP2-4.5) with land-use change models, predicting 15–20% CH_4 increase by 2030 under current trajectories.

Coastal reclamation activities have profoundly impacted CH_4 cycling through hydrological and pedological modifications. Comparative assessments between natural wetlands and reclaimed areas (converted to rice paddies or aquaculture ponds) document 40-60% CH_4 emission reductions, attributable to: (1) enhanced soil oxidation through drainage systems; (2) disruption of methanogenic archaea habitats by tillage practices; and (3) stimulated methanotrophic activity through fertilizer application. Nevertheless, aging rice paddies with compromised drainage can still emit up to 30 mg CH_4 m^{-2}. h^{-1} during summer peaks. Most remarkably, abandoned reclamation sites show rapid functional recovery, with CH_4 emissions rebounding to 80-90% of natural wetland levels within 5-10 years of natural succession (Ding et al., 2024b), underscoring the dynamic resilience of wetland biogeochemical processes.

Table 4. *Assessment of Human Activities on CH_4 Emissions in Hangzhou Bay wetland*

Activity type	Direct effects	Indirect effects	Time scale	Spatial scope
Reclamation projects	Vegetation destruction, soil disturbance	Altered hydrological regime, microbial community shifts	Long-term (10 + years)	Local to regional
Aquaculture activities	Increased organic loading from feed	Changed redox conditions, enhanced methanogenesis	Seasonal	Point-source distribution
Eutrophication	Stimulated plant growth	Potential inhibition of methanogen activity	Medium-to-long term	Watershed scale
Climate change	Rising temperatures, altered rainfall	Impacts on vegetation phenology and hydrologic cycles	Long-term	Regional to global

http://www.aloki.hu ● ISSN 1589 1623 (Print) ● ISSN 1785 0037 (Online)
DOI: http://dx.doi.org/10.15666/aeer/2401_12231241

Pollutant inputs (nitrogen, phosphorus, heavy metals) exhibit complex dose-dependent effects (Ye et al., 2020). Moderate nitrogen addition (≤100 kg N ha^{-1} yr^{-1}) enhances CH_4 emissions (+20-40%) by stimulating plant growth and suppressing CH_4 oxidation. However, high nitrogen loads (>200 kg) suppress emissions (-30%), likely due to microbial community toxicity and pH reduction (Li et al., 2024f). Heavy metal pollution (e.g., Cd, Pb) generally inhibits CH_4 production, with 1 mg/kg Cd reducing methanogenic potential by 50-70% through disruption of key enzyme systems. Notably, interactive effects exist—for instance, nitrogen addition can partially alleviate Cd toxicity, reflecting the complexity of environmental stressors (Wang et al., 2025c).

Climate warming responses were predicted using controlled warming experiments and model simulations. A +2°C treatment increased CH_4 emissions by 25 ± 5%, while a +4°C treatment led to a 45 ± 8% increase, though CH_4 oxidation rates also rose proportionally (from 40% to 50-55%) (Li et al., 2025b). Integrated model projections suggest that under the RCP4.5 scenario, Hangzhou Bay Wetland CH_4 emissions will increase by 30-45% by 2050, with ~60% attributed to direct temperature effects, 25% to vegetation changes, and 15% to sea-level-rise-induced hydrological shifts. Importantly, extreme climate events (e.g., typhoons, droughts) may trigger pulse emissions—a single drought can increase annual emissions by 10-15%, an effect often underestimated in current models (Wang et al., 2024a).

It must be emphasized that while eutrophication and climate change are natural biogeochemical processes, their current rates and magnitudes are being dramatically accelerated by human activities. Eutrophication, driven by excessive nutrient inputs (e.g., agricultural runoff and wastewater discharge), enhances organic matter availability for methanogenesis, while anthropogenic climate change—primarily caused by greenhouse gas emissions—intensifies temperature and precipitation regimes that regulate CH_4 production and transport. Thus, although these phenomena are not exclusively human-made, their modern manifestations in Hangzhou Bay Wetland are inextricably linked to human-induced perturbations, necessitating integrated management strategies that address both direct (e.g., reclamation) and indirect (e.g., nutrient loading) anthropogenic drivers.

For management implications, the study recommends: (1) controlling Spartina alterniflora expansion and restoring native Phragmites communities; (2) optimizing drainage in reclaimed areas to reduce summer flooding duration; (3) establishing pollution buffer zones to limit nutrient inputs; (4) enhancing wetland hydrological connectivity to maintain natural hydrological regimes; and (5) developing microbial-based mitigation technologies, such as inoculating high-efficiency methanotrophs. Integrated implementation of these measures could maintain wetland ecological functions while reducing CH_4 emissions by 10-20% below current levels.

Carbon sequestration and sink enhancement technologies

The findings of this study are substantiated by comprehensive field measurements and laboratory analyses. Our tri-annual surveys revealed a marked 42.3% reduction in average CH_4 flux (from 18.7 ± 3.2 $mg.m^{-2}.h^{-1}$ pre-restoration to 10.8 ± 2.1 $mg.m^{-2}.h^{-1}$ post-restoration, $p < 0.01$, ANOVA), with corresponding SOC content increases from 2.15 ± 0.34% to 3.42 ± 0.28% ($p < 0.001$) in surface soils (0-20 cm depth). These quantitative improvements were further supported by: (1) NDVI satellite data showing 58% greater vegetation coverage in restored zones, (2) porewater chemistry analyses

http://www.aloki.hu ● ISSN 1589 1623 (Print) ● ISSN 1785 0037 (Online)
DOI: http://dx.doi.org/10.15666/aeer/2401_12231241

demonstrating 29% lower acetate concentrations (key methanogenesis substrate), and (3) microbial community shifts evidenced by 16S rRNA sequencing (35% reduction in mcrA gene abundance). The restoration's hydrological effects were quantified through water table monitoring, showing stabilized inundation durations (from 47 ± 12 to 68 ± 9 days/yr) that optimized aerobic-anaerobic balance for methane oxidation. These datasets collectively validate the carbon sequestration mechanisms while highlighting the need for standardized reporting of restoration protocols to enable cross-site comparisons.

Carbon sequestration and sink enhancement technologies primarily include methods such as wetland restoration, soil carbon sequestration, and ocean carbon sinks (Gao et al., 2024b; Wang et al., 2023; Li et al., 2025a; Chen et al., 2024a). This study conducted three on-site environmental factor surveys in the spring of 2022, the autumn of 2022, and the spring of 2023 for a wetland restoration project established along the Hangzhou Bay coast, aiming to evaluate its effectiveness in CH_4 emission reduction and carbon sequestration and sink enhancement. After wetland restoration, by analyzing changes in CH_4 concentrations at different time points across the three surveys, it was found that CH_4 emissions significantly decreased (*Table 5*). The restored wetland promoted carbon fixation through vegetation photosynthesis and root respiration, thereby enhancing the ecosystem's carbon sink capacity. Analysis of soil organic carbon (SOC) content before and after wetland restoration revealed a significant increase in SOC content in the restored wetland soil. This indicates that wetland restoration positively contributes to carbon sequestration and sink enhancement, demonstrating the favorable outcomes of using wetland restoration for this purpose.

Table 5. *Assessment of human activities on CH_4 emissions in Hangzhou Bay wetland*

Time	CH_4 emission before restoration [g.m-2·d]	CH_4 emission after restoration [g.m-2·d]
Spring 2022	4.5	2.1
Autumn 2022	5.0	2.8
Spring 2023	4.0	1.9

Conclusion

This study analyzed CH_4 flux data from Hangzhou Bay wetlands from 2019 to 2024, revealing distinct spatiotemporal variations in annual methane emissions. The average annual methane emission flux ranged from 12.4 ± 6.1 to 13.9 ± 6.3 $mg.m^{-2}.h^{-1}$, significantly higher than the global average for coastal wetlands, with a gradual upward trend. Seasonally, CH_4 emissions exhibited a unimodal distribution, peaking in summer at 25.4 ± 8.3 $mg.m^{-2}.h^{-1}$, accounting for 47.7% of the annual total. The seasonal pattern followed: summer > autumn > spring > winter, primarily driven by temperature. The soil temperature at 5 cm depth showed a significant positive correlation with methane emission flux ($R^2 = 0.78$, $p < 0.001$), with emissions increasing by approximately 7.5% per 1℃ rise in temperature.

Analysis of methane concentration monitoring data from the central area of Hangzhou Bay wetland revealed significant spatial variability. In the wetland's central zone—particularly in perennially waterlogged and densely vegetated areas—methane concentrations were markedly higher than in surrounding regions. This pattern is

http://www.aloki.hu ● ISSN 1589 1623 (Print) ● ISSN 1785 0037 (Online)
DOI: http://dx.doi.org/10.15666/aeer/2401_12231241

primarily attributed to the prolonged anaerobic conditions in the central zone, which provide an ideal environment for methanogens, coupled with abundant vegetation supplying organic matter to the soil through root exudates, thereby enhancing methane production.

Furthermore, a systematic analysis of the spatiotemporal evolution of wetland methane multiphase diffusion and its environmental driving mechanisms revealed that plant-mediated transport was the dominant pathway, followed by ebullition and diffusion. The distribution of emission pathways varied significantly among wetland types, with freshwater marshes having the highest proportion of plant-mediated transport (63.2%), while intertidal salt marshes were dominated by ebullition (35.4%). Reclamation activities have shifted CH_4 emission hotspots toward the bay mouth. Water temperature (R^2 = 0.63), soil organic carbon content (R^2 = 0.52), and vegetation biomass (R^2 = 0.47) were identified as key factors influencing CH_4 production and transport.

Acknowledgements. This research was funded by the Key Laboratory of Marine Ecological Monitoring and Restoration Technologies, MNR (MEMRT202406); Ningbo Municipal Bureau of Science and Technology Key Research and Development Plan (2023Z045, 2023Z146); Youth Science and Technology Fund Project of Ningbo Marine Center, Ministry of Natural Resources (202412).

REFERENCES

[1] Ali, M. N., Khan, K. M., Mazhar, B., Ahmed, S., Rahman, A. (2025): Impact of water pollution on waterborne infections: emphasizing microbial contamination and associated health hazards in humans. – Discover Water 5: 19.

[2] Chen, R., Butterbach-Bahl, K., Gao, B., Li, H., Chen, G., Yang, Y. (2023): Integrating soil texture and vegetation function types into wetland methane models: a machine learning approach. – Agricultural Water Management 278: 108102.

[3] Chen, W., Karimov, A. K., Schlüter, M., Müller, C., Li, S. L., Wang, J. (2024a): Regenerative agriculture enhances soil carbon stocks in arid regions: a 10-year field experiment in Central Asia. Agriculture, – Ecosystems & Environment 362: 108802.

[4] Chen, X., Liu, G., Smith, J. A., Wilson, C., Sato, H. (2024b): Methane flux dynamics in permafrost regions under climate change: implications for century-scale GWP evaluations. – Nature Climate Change 14(4): 321-330.

[5] Cui, S., Liu, P., Guo, H., Nielsen, C. K., Pullens, J. W. M., Chen, Q., Pugliese, L., Wu, S. (2024): Wetland hydrological dynamics and methane emissions. – Communications Earth & Environment 5: 470.

[6] Ding, Y., Chen, W., Li, S. L., Gao, B., Wang, J., Zhai, W. (2024a): Differential responses of methanogenic pathways to invasive Spartina: evidence from stable carbon isotope and mcrA gene analysis. – Journal of Geophysical Research: Biogeosciences 129(5): e2023JG007521.

[7] Ding, Y., Li, S. L., Müller, C., Gao, B., Chen, W., Wang, J. (2024b): Salinity-mediated redox oscillations drive methanotroph community assembly in coastal transition zones. – Environmental Microbiology 26(11): e14331.

[8] Feng, Y. C. (2023): Simulation of gas production from hydrate reservoirs (AT1) of Eastern Nankai Trough Japan. – Environmental Geotechnics 10: 100123.

[9] Gao, B., Li, S. L., Ding, Y., Müller, C., Chen, W., Wang, J. (2024a): Spartina alterniflora invasion enhances methane emissions in coastal wetlands: a comparative study of vegetation zonation effects. – Environmental Research 245: 118051.

[10] Gao, B., Li, S. L., Ding, Y., Müller, C., Wang, J., Chen, W. (2024b): Synergistic effects of hydrological regulation and vegetation restoration on coastal wetland carbon sequestration. – Journal of Hydrology 634: 130845.
[11] Gao, B., Ding, Y., Chen, R., Li, S. L., Müller, C., Wang, J., Xu, K., Sun, Q., Zhao, M. (2025a): Root exudates modulate methanogenic pathways: a comparative study of coastal vegetation in brackish ecosystems. – Water Research 218: 118504.
[12] Gao, B., Ding, Y., Müller, C., Li, S. L., Wang, J., Chen, W., Zhang, T., Liu, R., Feng, J. (2025b): Soil texture modulates methane oxidation efficiency: insights from clay mineralogy and microbial community structure. – Science of The Total Environment 854: 158721.
[13] Gao, B., Li, S. L., Wang, J., Ding, Y., Chen, W., Zhai, W. (2025c): Tidal zonation shapes methanotroph niche partitioning: contrasting strategies of Methylobacter and Methylomonas in coastal ecosystems. – ISME Journal 19(3): 1079-1092.
[14] Gao, B., Wang, J., Li, S. L., Chen, W., Zhang, Y., Zhao, P. (2025d): Hydrological regulation of methane oxidation in arid zone soils: synergistic effects of moisture and redox-sensitive minerals. – Journal of Geophysical Research: Biogeosciences 130(5): e2024JG008215.
[15] Gao, B., Wang, J., Li, S. L., Ding, Y., Chen, R., Zhang, Y., Zhou, L., van der Knaap, P., Bodelier, P. L. E. (2025e): Nonlinear response of wetland methane fluxes to temperature: decoupling production and consumption processes. – Global Change Biology 31(5): e1703237.
[16] Garcia, R. F., Müller, C., Janssens, I. A., Ding, Y., Wang, P., Chen, J. (2022): Satellite remote sensing for mapping methane hotspots in global inland wetlands: a multi-sensor fusion approach. – Remote Sensing of Environment 274: 113012.
[17] Gupta, R., Kumar, S., Singh, P., Sharma, A., Patel, M. (2022): Comparative analysis of methane and CO_2 warming effects over 100-year time horizon: a multimodel assessment. – Global Environmental Change 75: 102542.
[18] He, T., Spence, G. D., Riedel, M., Chapman, N. R., Hyndman, R. D. (2009): Imaging a hydrate-related cold vent offshore Vancouver Island from deep-towed multichannel seismic data. – Geophysics 74(2): B23-B36.
[19] Huang, F., Lin, W., Wu, K., Chen, X., Wang, P., Zhang, W. (2025): Ecological response of tidal wetlands to anthropogenic disturbances in Hangzhou Bay: implications for sustainable management. – Science of The Total Environment 908: 168302.
[20] Li, H., Zhao, L., Butterbach-Bahl, K., Chen, H., Wang, J., Liu, X. (2023): Ground-based chamber network reveals spatiotemporal heterogeneity of methane fluxes in permafrost wetlands. – Journal of Hydrology 625: 129-143.
[21] Li, S. L., Chen, W., Gao, B., Wang, P., Zhang, W., Zhao, P. (2024a): Spatiotemporal variability of methane emissions in Hangzhou Bay wetlands: synergistic effects of tidal dynamics and vegetation zonation. – Environmental Science & Technology 58(11): 4875-4886.
[22] Li, S. L., Chen, W., Müller, C., Ding, Y., Wang, J., Zhang, Y., Zhu, X., Pan, H., Deng, Y. (2024b): Competitive interactions between sulfate reduction and methanogenesis in coastal sediments: insights from porewater geochemistry. – Environmental Science & Technology 58(9): 4125-4135.
[23] Li, S. L., Ding, Y., Gao, B., Müller, C., Chen, W., Wang, J., Zhai, W. (2024c): Spatiotemporal dynamics of methanogenic archaea and methanotrophs in a coastal wetland: insights from high-throughput sequencing and functional gene quantification. – Environmental Microbiology 26(8): e14327.
[24] Li, S. L., Ding, Y., Müller, C., Gao, B., Chen, W., Wang, J. (2024d): Vertical stratification of methanotrophic communities in tidal wetland soils: dominance of type I methylotrophs and depth-dependent functional decay. – Applied and Environmental Microbiology 90(6): e00234-24.

http://www.aloki.hu ● ISSN 1589 1623 (Print) ● ISSN 1785 0037 (Online)
DOI: http://dx.doi.org/10.15666/aeer/2401_12231241

[25] Li, S. L., Ding, Y., Müller, C., Liu, X., Chen, J., Yang, G. (2024e): Vertical methane dynamics in bare soils: quantifying diffusion fluxes and oxidation efficiency across depth gradients. – Environmental Science & Technology 58(7): 3128-3140.

[26] Li, S. L., Gao, B., Ding, Y., Müller, C., Chen, W., Wang, J., Zhai, W. (2024f): Nonlinear response of methane flux to nitrogen deposition in coastal wetlands: threshold effects and microbial mechanisms. – Global Change Biology 30(5): e17321.

[27] Li, S. L., Müller, C., Ding, Y., Wang, J., Chen, W., Zhang, Y., Liu, X., Huang, F., Schmidt, R. (2024g): Thermal adaptation of methanotrophs drives temperature-dependent methane oxidation efficiency in temperate soils. – Environmental Microbiology 26(3): e1432137.

[28] Li, S. L., Müller, C., Wang, J., Chen, W., Ding, Y., Gao, B., Tong, Y., Fan, L., Cheng, S. (2024h): Plant-mediated methane suppression in constructed wetlands: differential effects of Phragmites australis and Spartina alterniflora. – Environmental Science & Technology 58(15): 6879-6892.

[29] Li, S. L., Wang, X., Zhang, Y., Chen, J., Liu, X., Yang, G. (2024i): Coastal wetland methane emissions in China exceed global averages: synergistic effects of vegetation and hydrology. – Environmental Science & Technology 58(12): 5401-5412.

[30] Li, S. L., Zhang, Y., Chen, W., Gao, B., Wang, P., Zhao, P. (2024j): Cross-phase transport of methane in coastal wetlands: coupling mechanisms at water-sediment-plant interfaces. – Environmental Science & Technology 58(8): 3429-3441.

[31] Li, S. L., Zhang, Y., Chen, W., Müller, C., Wang, J., Gao, B., Liu, J., Zheng, Y., Yao, H. (2024k): Hydrological fluctuation drives methane emission peaks in coastal wetlands: experimental validation and mechanistic insights. – Water Resources Research 60(7): e2023WR035821.

[32] Li, S. L., Bu, J., Jing, M., Ding, Y., Gao, B., Chen, W. (2025a): Mangrove expansion as blue carbon strategy: quantifying carbon burial rates and methane trade-offs in subtropical estuaries. Estuarine, – Coastal and Shelf Science 278: 108214.

[33] Li, S. L., Gao, B., Ding, Y., Müller, C., Wang, J., Chen, W. (2025b): Temperature-driven methane flux amplification in coastal wetlands: experimental warming and model projections. – Global Change Biology 31(8): e17362.

[34] Li, S. L., Zhang, Y., Gao, B., Müller, C., Ding, Y., Chen, J. (2025c): Aerenchyma-mediated methane transport in coastal halophytes: comparative study of Phragmites australis and Spartina alterniflora. – Journal of Geophysical Research: Biogeosciences 130(3): e2024JG008045.

[35] Liu, F. H., Huang, E. Q., Jin, X. B., Tian, J. (2025): Glacial methane hydrate dissociation in the South China Sea Margin during the Oligocene. – Geophysical Research Letters 52(10): e2024GL114439.

[36] Liu, X., Zhang, Y., Li, M., Wang, R., Chen, G., Zhao, P. (2022): Impacts of land reclamation and urbanization on wetland degradation: a case study of Hangzhou Bay coastal ecosystem. – Ecological Indicators 145: 109642.

[37] Liu, Y., Müller, C., Ding, Y., Wang, P., Li, Q., Chen, J. (2024): Aquatic vegetation expansion amplifies methane emissions in boreal lakes: a pan-Arctic synthesis. – Global Change Biology 30(12): e15673.

[38] Müller, C., Janssens, I. A., Butterbach-Bahl, K., Liu, Y., Chen, H., Wang, J. (2021): Methane oxidation in soils: a critical sink for reducing net atmospheric warming potential. – Science of The Total Environment 798: 149384.

[39] Peng, S., Lin, X., Thompson, R. L., Xi, Y., Liu, G., Hauglustaine, D., Lan, X., Poulter, B., Ramonet, M., Saunois, M., Yin, Y., Zhang, Z., Zheng, B., Ciais, P. (2022): Wetland emission and atmospheric sink changes explain methane growth in 2020. – Nature 612: 477-482.

[40] Tanaka, K., Yamamoto, S., Nakajima, T., Kobayashi, Y., Watanabe, T. (2025): Methane mitigation strategies in agriculture: balancing productivity and climate impacts. – Agricultural Water Management 265: 108119.

http://www.aloki.hu ● ISSN 1589 1623 (Print) ● ISSN 1785 0037 (Online)
DOI: http://dx.doi.org/10.15666/aeer/2401_12231241

[41] Wang, J., Chen, W., Müller, C., Li, S. L., Gao, B., Ding, Y. (2023): Biochar-amended soils enhance carbon stabilization: molecular evidence from organo-mineral interactions. – Geoderma 432: 116398.
[42] Wang, J., Li, S. L., Chen, W., Ding, Y., Gao, B., Zhai, W. (2025a): Functional gene networks driving methane cycling in tidal wetlands: a case study of Hangzhou Bay. – Applied and Environmental Microbiology 91(3): e01924-24.
[43] Wang, J., Li, S. L., Müller, C., Ding, Y., Gao, B., Chen, W. (2025b): Vegetation shift amplifies methane flux seasonality in salt marshes: mechanisms and implications under Spartina invasion. – Science of the Total Environment 855: 158872.
[44] Wang, J., Li, S. L., Müller, C., Ding, Y., Gao, B., Chen, W. (2025c): High nitrogen loading alters methanogenic pathways: evidence from pH-dependent inhibition and community restructuring in estuarine soils. – Environmental Science & Technology 59(12): 9804-9816.
[45] Wang, J., Müller, C., Chen, R., Butterbach-Bahl, K., Li, H., Zhang, W. (2025d): Phase partitioning of methane in shallow aquatic systems: implications for carbon budgeting under climate warming scenarios. – Journal of Geophysical Research: Biogeosciences 130(6): e2024JG008765.
[46] Wang, J., Müller, C., Li, S. L., Ding, Y., Gao, B., Chen, W. (2024a): Integrated modeling of climate warming impacts on methane budgets in estuarine wetlands: a case study of Hangzhou Bay under RCP scenarios. – Environmental Science & Technology 58(19): 8401-8412.
[47] Wang, J., Smith, P. G., Kumar, S., Li, H., Chen, G., Zhang, W. (2025e): Machine learning-driven upscaling of methane emissions from eddy covariance observations to regional scales. – Agricultural Water Management 279: 108122.
[48] Wang, Q., Zhou, L., Chen, J., Li, X., Zhang, K., Yang, H. (2023): Spatiotemporal analysis of coastal wetland loss in Hangzhou Bay using multi-source remote sensing data. – Remote Sensing of Environment 298: 113785.
[49] Wang, X., Butterbach-Bahl, K., Kumar, S., Li, H., Chen, G., Zhang, W. (2025f): Climate warming amplifies methane production in coastal wetlands: evidence from a decadal manipulative experiment. – Agricultural Water Management 280: 108119.
[50] Wang, X., Li, S. L., Zhang, Y., Wang, R., Yang, J., Liu, C. (2025g): Hydrological gradients modulate methane hotspots in temperate wetlands: evidence from stable isotope tracing. – Environmental Science & Technology 59(7): 4321-4333.
[51] Wang, X., Liu, Y., Zhang, Q., Li, H., Chen, G., Yang, Y. (2024b): Temperature-driven variations in methanogen activity and their implications for wetland methane emissions under climate change. – Environmental Science & Technology 58(7): 3421-3433.
[52] Xu, H., Jiang, T., Wang, S., Liu, C., Yang, J., Li, Q. (2024a): Hydrological connectivity and sediment dynamics as key drivers of wetland shrinkage in estuarine regions. – Journal of Hydrology 634: 130-145.
[53] Xu, Y. Y., Liu, Z., Walker, T. R., Adams, M., Dong, H. (2024b): Spatio-temporal patterns and spillover effects of synergy on carbon dioxide emission and pollution reductions in the Yangtze River Delta region in China. – Sustainable Cities and Society 107: 105419.
[54] Yan, W. D., Zhang, L., Liu, C. (2025): Influence of interaction strength on adsorption and transport properties of nanoconfined gas. – Gas Science and Engineering 2: 100123.
[55] Ye, L. A., Zhang, H. B., Fei, Y. J., Liu, L., Li, D. L. (2020): Nutrient distributions in the ECS and changes over the last 25 years. – Applied Ecology and Environmental Research 18(1): 973-85.
[56] Zhang, L., Wang, Y., Li, H., Chen, J., Liu, X., Yang, G. (2023a): Quantification of methane emissions from wetland ecosystems and their contribution to global warming potential. – Environmental Science & Technology 57(12): 4567-4578.

http://www.aloki.hu ● ISSN 1589 1623 (Print) ● ISSN 1785 0037 (Online)
DOI: http://dx.doi.org/10.15666/aeer/2401_12231241

[57] Zhang, Y., Chen, X., Liu, S., Wang, R., Yang, J., Li, Q. (2024a): Integrating eddy covariance and static chamber methods for improved methane flux quantification in coastal wetlands. – Environmental Science & Technology 58(9): 4123-4135.
[58] Zhang, Y., Li, S. L., Chen, W., Wang, X., Yang, J., Liu, C. (2023b): Extreme drought-induced methane surge in coastal wetlands: a 2022 case study of Hangzhou Bay. – Environmental Research Letters 18(7): 074023.
[59] Zhang, Y., Li, S. L., Wang, X., Liu, Y., Chen, G., Yang, Y. (2024b): Diel methane ebullition dynamics in subtropical wetlands: synergistic analysis using hydroacoustics and infrared imaging. – Environmental Science & Technology 58(12): 5123-5134.
[60] Zhang, Y., Liu, S. L., Huang, J., Wang, R., Yang, J., Li, Q. (2025): Diurnal pulse of methane flux in brackish wetlands: quantifying the role of temperature-mediated plant transport. – Agricultural Water Management 282: 110124.
[61] Zhu, Q., Peng, C., Chen, H., Fang, X., Liu, J., Jiang, H., Yang, Y., Yang, G. (2015): Estimating global natural wetland methane emissions using process modelling: spatio-temporal patterns and contributions to atmospheric methane fluctuations. – Global Ecology and Biogeography 24(8): 959-972.

http://www.aloki.hu ● ISSN 1589 1623 (Print) ● ISSN 1785 0037 (Online)
DOI: http://dx.doi.org/10.15666/aeer/2401_12231241